

PROPERTIES OF P-TYPE SnS THIN FILMS PREPARED BY CHEMICAL BATH DEPOSITION

E. GUNER^a, F. GODE^c, C. ULUTAS^b, F. KIRMIZIGUL^b, G. ALTINDEMIR^b,
C. GUMUS^{b*}

^aDepartment of Primary Education, University of Erziyes 33039 Kayseri, Turkey

^bPhysics Department, University of Cukurova 01330 Adana, Turkey

^cPhysics Department, University of Mehmet Akif Ersoy 15100 Burdur, Turkey

Thin film of tin monosulfide (SnS) is deposited onto glass substrates using chemical bath deposition (CBD) at room temperature for 24 h. The structural, electrical, and optical properties of the film are determined using X-ray diffraction (XRD), energy-dispersive X-ray (EDX), scanning electron microscopy (SEM), Hall Effect measurement and spectrophotometry. Obtained films were polycrystalline of an orthorhombic structure. The crystallite size, lattice parameters, defective location density, and texture coefficient of the film are calculated from the XRD data. EDX analysis revealed that thin film has a nearly stoichiometric composition (Sn/S, 54.13/45.8). From the Hall Effect measurement, it was found that SnS thin film exhibits p-type conduction. Its resistivity and mobility were calculated to be $2.53 \times 10^5 \Omega \cdot \text{cm}$ and $8.99 \times 10^5 \text{ cm}^2/\text{V} \cdot \text{s}$ respectively. The activation energy is calculated to be 0.527 eV in temperature range from 353-573 K by Arrhenius equation. Optical band gap values of direct and indirect transitions are estimated to be 1.37 eV and 1.05 eV, respectively.

(Received December 8, 2010; accepted December 22, 2010)

Keywords: SnS, Chemical bath deposition, Thin films

1. Introduction

In recent years, thin films of SnS have attracted much attention for the photovoltaic applications due to the high absorption coefficient ($\approx 10^4 \text{ cm}^{-1}$ near the fundamental edge) [1, 2] and high conductivity (hole mobility = $90 \text{ cm}^2 \text{ V}^{-1} \text{ s}^{-1}$). SnS belongs to groups IV-VI of compounds formed with Sn as the cation and S as the anion. The constituent elements are inexpensive, nontoxic and abundant in nature leading to the development of devices that are environmentally safe and have public acceptability. SnS is an important optoelectronic material that is found in zinc blend with the lattice constant ($a = 0.5845 \text{ nm}$) [3], orthorhombic with the lattice constants ($a = 0.385 \text{ nm}$, $b = 1.142 \text{ nm}$ and $c = 0.438 \text{ nm}$) [4, 5] and herzenbergite [6] crystal structures. SnS shows a p-type electrical conductivity and its electrical conductivity can be controlled by using different dopants like Al, Ag and Cl. The optical properties of SnS vary depending on the synthesizing or fabrication method, but most work agrees with direct (1.2-1.5 eV) and indirect (1.0-1.2 eV) band gap values. These properties enable SnS thin films to be used as an absorption layer in the fabrication of heterojunction solar cell [4, 7]. SnS thin films can be generated by many methods such as thermal evaporation [8], pulse electrodeposition [9], spray pyrolysis [10], SILAR [11], electron beam evaporation [12], chemical bath deposition [13]. The film in this study is grown by chemical bath deposition (CBD) which creates a thin film on a solid substrate via a reaction in a liquid solution. The CBD method is inexpensive, easy to prepare and its necessary vessels can be found in an ordinary chemistry laboratory. Therefore, this method has many advantages over others used to grow semiconductor thin films.

*Corresponding author: cgumus@cu.edu.tr

In this work, we report on the structural, morphological and optical properties of SnS thin films by CBD. Moreover, we present the activation energy value from the temperature-dependent current measurement. An analysis of the published data indicates that little is known about the room temperature synthesis of SnS thin films. Because of this reason, an attempt has been made to deposit SnS thin films using precursors in homogenous phase at room temperature in the present work. So we have obtained a better crystal structure at room temperature compared with other works in which SnS thin films were obtained by CBD at room temperature.

2. Experimental

2.1. Fabrication of SnS thin films

The precursor compounds and their concentrations have a strong influence on obtaining a well adherent film on the substrate, so each compound used to deposit SnS thin film was diligently selected. For a Sn source $\text{SnCl}_2 \cdot 2\text{H}_2\text{O}$ is preferred rather than $\text{SnCl}_4 \cdot 5\text{H}_2\text{O}$. This preference is due to $\text{SnCl}_2 \cdot 2\text{H}_2\text{O}$ being cheaper and containing 52.9 % Sn, compared to the 33.9 % Sn in $\text{SnCl}_4 \cdot 5\text{H}_2\text{O}$. In this experimental process, three different sulphur sources such as thioacetamide (TA), $(\text{Na}_2\text{S}_2\text{O}_3)$ and thiourea (CSN_2H_4) with different concentrations are used. When $\text{Na}_2\text{S}_2\text{O}_3$ and CSN_2H_4 were present in the solution as a S source, precipitation occurred very rapidly. As a result, the film was not formed on the substrate. Accordingly, TA was preferred as a S source.

In order to obtain high quality thin films by CBD, the reaction must be very slow. Triethanolamine (TEA) is used to help Sn come into existence in solution by reducing the reaction speed. When TEA was not in the solution, the precipitation was very rapid and the film did not form on the substrate. Trisodium citrate (TSS) and EDTA salts were employed as complexing agents maintaining the other variables. TSS was used as a complexing agent because the films obtained from the solution prepared with TSS have given better results compared to the ones from the solution prepared with EDTA salt. The buffer was used to fix the pH value to 10.7 during the experiment.

SnS thin film was prepared by first mixing 5 ml of 1 M $\text{SnCl}_2 \cdot 2\text{H}_2\text{O}$, 10 ml of 3.75 M triethanolamine (TEA) $[\text{N}(\text{CH}_2\text{CH}_2\text{OH})_3]$, 5 ml ammonia/ammonium chloride ($\text{NH}_3/\text{NH}_4\text{Cl}$, pH=10.7) buffer solution, 5 ml of 0.66 M tri-sodium citrate (TSS) ($\text{C}_6\text{H}_5\text{Na}_3\text{O}_7$), 5 ml of 1 M thioacetamide (TA) $[\text{CH}_3\text{CSNH}_2]$, and the rest was completed with deionized water to make the total volume of the solution 100 ml. This solution was poured in a glass vessel which had previously been rinsed with deionized water and then left to soak for a short period of time in 10 ml of nitric acid solution. Before the amorphous glass substrates (76mm \times 26mm \times 1mm) were put into the solution, they were subjected to the following cleaning process: cleaned with detergent, soaked in diluted acid, rinsed in deionized water, soaked for 3 min in isopropyl alcohol, rinsed in deionized water and then dried in air. The substrates were put in glass vessels vertically. The deposition is made at room temperature (27 °C) for 24 h. The colour of the solution which forms SnS thin films was observed to turn into milk white, yellow and then a chocolate colour. Many researchers forming SnS thin films have observed a chocolate colour [14]. The deposition rate of SnS thin films was ~ 21.67 nm/h.

2.2. Characterization techniques of SnS thin films

The structural analysis of the films were performed using a Rigaku RadB diffractometer (XRD) with a CuK_α line ($\lambda=1.5405 \text{ \AA}$) with 2θ ranging from 20° to 70°. Picture of surface morphology and elemental composition of SnS thin film were determined by using an EVO40-LEO computer controlled digital scanning electron microscope attached with the EDX system. Electrical parameters like mobility, resistance and the type of electrical conduction were determined by performing Hall measurement at room temperature. A Hall Effect Measurement System (HS-3000 with Manual Ver 3.5) was used for these measurements. In order to determine the optical characterization of the thin film deposited, optic transition spectrum measurement was performed at room temperature and recorded using a Perkin Elmer UV/VIS Lambda 2S

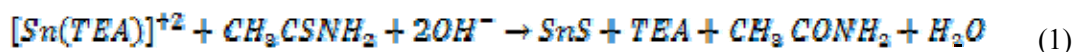
spectrometer for the wavelength range 190-1100 nm. The thickness of the film deposited was measured using a thin film measurement system (Filmetrics F30).

3. Results and discussion

3.1. Deposition mechanism

The least known aspect of SnS thin film grown by using CBD is probably how the film is formed on the substrate. It is thought that three processes are effective in forming the film; ion-ion, hydroxide aggregation and complex-decomposition mechanisms. At ion-ion mechanism, Sn and S ions diffuse to the substrate to constitute the SnS nucleus. SnS nucleuses grow through Sn and S ions absorbed from the solution. SnS crystals are connected to each other and the substrate by van der Waals forces. The growth of SnS crystals continues until the precursors in the solution finish. At hydroxide aggregation mechanism, hydroxide colloidal particles diffuse to the substrate and adhere to the substrate then they react with S ions, this reaction leads to an exchange between sulphide and hydroxide ions and it may occur both on the surface and in the solution. Finally, the first particles of SnS adhere to each other to form an aggregated film. At complex-decomposition mechanisms, the complex (Sn-L, where L is a ligand) decomposes to SnS on the substrate and the process continues to make up a film of aggregated crystal [15]. It must be kept in mind that the mechanisms may vary during the formation of the film.

It is required to secure the reaction in the solution to be realized slowly to obtain a quality film by CBD. In order to prevent a solid compound to be formed from rapid precipitation, metal ions can make a complex with a ligand. It can be inferred from this reaction that film formation can occur not only by simple ion-by-ion or cluster mechanism, but also by complex mechanisms [15]. The SnS is formed when the ionic product of Sn^{+2} and S^{-2} ions exceeds the solubility product of SnS and, thus the concentration of tin and sulphur ions have to be controlled very carefully during the growth. The kinetics of formation of SnS films can be understood from following reaction [13]:



It was accepted that Sn^{+2} ions made bonds with TEA ligand to form Sn[TEA] at first during deposition, that undesirable materials like $[\text{Sn}(\text{OH})_2]$ were prevented from precipitation thanks to this complex and that also at further stage the complex broke to make bonds with S^{-2} ions and SnS compound formed.

3.2. Structural properties of SnS thin films

The X-ray diffraction pattern of SnS thin film deposited on an amorphous glass substrate at 27 °C for 24 h is shown in Fig. 1. Three peaks corresponding to the diffraction of orthorhombic SnS (PDF card no: 39-0354) appear clearly in the figure. This shows that the deposited film has a polycrystalline nature and good crystalline structure because of sharp structural peaks. Figure exhibits three peaks at angular position $2\theta = 21.741^\circ$ for the first one, corresponding to (110) plane ($d = 4.084 \text{ \AA}$), $2\theta = 26.880^\circ$ for the second one, corresponding to (021) plane ($d = 3.314 \text{ \AA}$) and $2\theta = 31.370^\circ$ for the third one, corresponding to (111) plane ($d = 2.849 \text{ \AA}$) of the orthorhombic phase of SnS.

It should be noted that from the XRD result, polycrystalline SnS film was obtained on glass substrate at room temperature. This result is better than Ref. [16-18], in which the XRD analysis showed that deposited SnS thin films onto glass substrates were of low crystallinity. Moreover, Ref. [19] and Ref. [20] reported that chemically deposited SnS films at 80 °C on glass and on $\text{SnO}_2/\text{glass}$ substrates present an amorphous structure. It can be observed that there is a peak at 2θ value of 23.920° originating from (111) plane of Sn (PDF card no: 5-0390). This shows

that there is an existence of crystalline tin in the deposited film. The existence of crystalline tin may result from more tin than necessary being present in the solution.

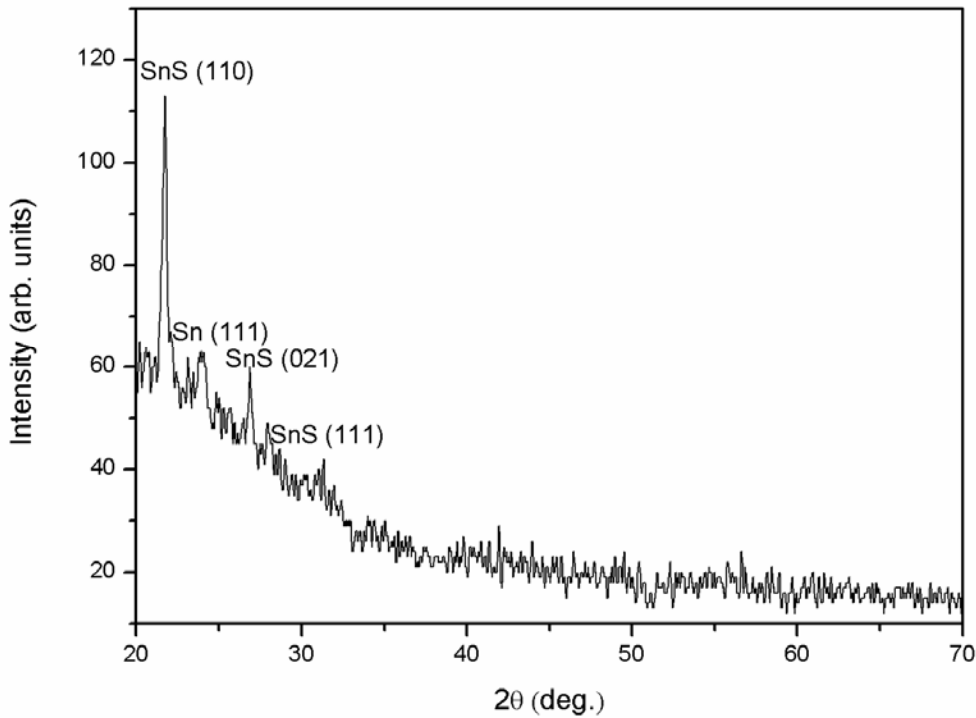


Fig. 1. X-ray diffraction pattern of SnS thin film deposited at 27 °C for 24 h.

The lattice plane index (hkl), interplanar distance d_{hkl} and lattice parameters have the following relationships for orthorhombic crystal [21]:

$$\frac{1}{d_{hkl}^2} = \frac{h^2}{a^2} + \frac{k^2}{b^2} + \frac{l^2}{c^2} \quad (2)$$

According to the data of the XRD peaks, we calculated the lattice parameters (a , b and c) of the SnS film. The evaluated lattice parameters of the SnS film are $a = 4.343 \text{ \AA}$, $b = 11.995 \text{ \AA}$ and $c = 3.976 \text{ \AA}$.

An estimation of the grain size of the polycrystalline SnS film was obtained from the broadening of the XRD peaks according to the Scherrer's formula [22]:

$$D = \frac{0.9\lambda}{\beta \cos \theta} \quad (3)$$

where D is the grain size, λ is the wavelength of the Cu- K_α radiation used ($\lambda = 1.5405 \text{ \AA}$), β is experimentally observed diffraction peak width at half maximum intensity (FWHM), θ is the Bragg angle.

For the fabrication of good quality thin film to use in optical devices, it is necessary to reduce the surface roughness and dislocation density of the SnS film. So the value of the dislocation density (δ) which gives the number of defects in the film was calculated from the average values of the crystallite size D by the relationship [23]:

$$\delta = \frac{1}{D^2} \quad (4)$$

The (hkl) plane, FWHM value, grain size (D) and dislocation density (δ) values of SnS thin film are listed in Table 1. In order to characterize a material exactly, its crystal structure, lattice parameters, size, shape and preference orientation of its grains must be known; therefore, the texture coefficient was determined in order to find preferential orientation of crystals in deposited polycrystalline material. The texture coefficient is one of the basic structure parameters in all polycrystalline materials. So texture coefficient was calculated from the x-ray diffraction result by using the equation:

$$T_{c(hkl)} = \frac{I_{(hkl)}/I_{o(hkl)}}{1/N \sum_n I_{(hkl)}/I_{o(hkl)}} \quad (5)$$

where $T_{c(hkl)}$ is the texture coefficient of (hkl) plane, $I_{(hkl)}$ is the intensity measured for (hkl) plane, $I_{o(hkl)}$ is the intensity of (hkl) plane taken from standard data in PDF card fitting in the x-ray diffraction pattern of material, n is the diffraction peak number and N is the total reflection number. For a film to have a preferential orientation at any (hkl) plane, the texture coefficient must be at least one. The calculated texture coefficient values of SnS thin film for different (hkl) planes are shown in Table 1. As seen from Table 1 the preferential orientation of the deposited film was (110) plane. This denotes that the number of grains along this plane is more than the other planes.

Table 1. (hkl) plane, FWHM value, grain size (D), dislocation density (δ) and texture coefficient ($T_{c(hkl)}$) values of SnS thin film.

(hkl)	FWHM	D (Å)	δ ($\times 10^2 \text{ nm}^{-2}$)	$T_{c(hkl)}$
(110)	0.346	246	0.165	2.148
(021)	0.293	296	0.114	0.568
(111)	0.352	244	0.168	0.284

3. 3. Surface morphology of SnS thin films

The SEM picture of SnS thin film deposited at 27 °C for 24 h is shown in Fig. 2. It was seen that the film had a needle shape grain structure without cracks on the surface. The grains crystallization was relatively good, grain sizes were almost near and the surface was uniformly covered. Surface properties observed have a strong effect on the optical properties of the thin film such as transition, absorption, and reflection. When such a surface morphology is formed on the surface of gas sensor or super condenser, it provides an extensive surface area for reaction [24].

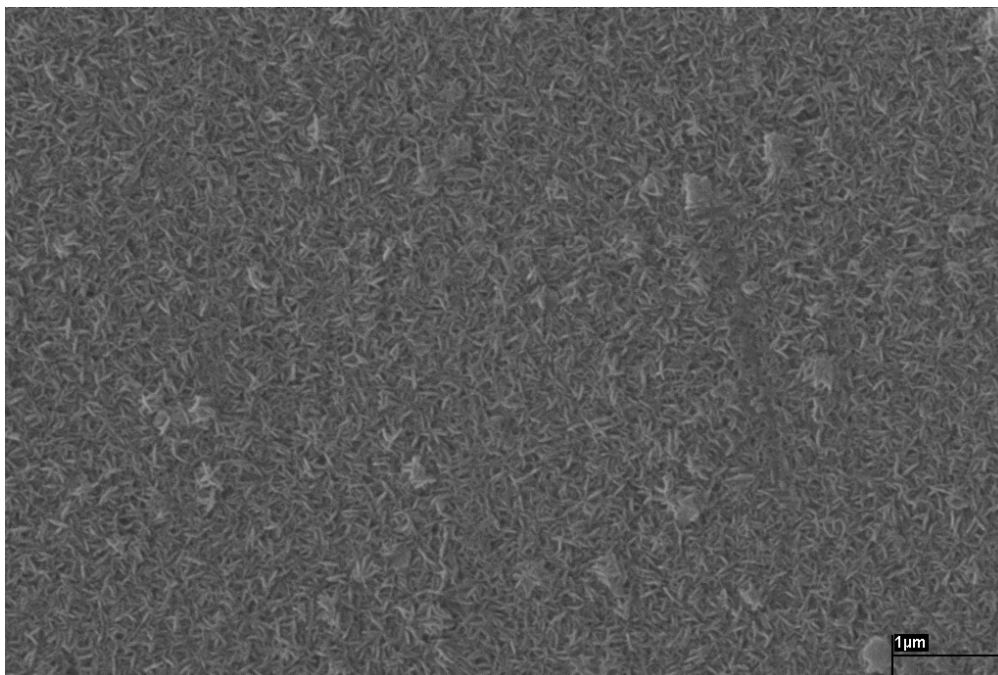


Fig. 2. SEM picture of SnS thin film deposited at 27 °C for 24 h.

3. 4. EDX analysis of SnS thin films

EDX technique was used to determine the composition of SnS thin film. Fig. 3 shows the EDX spectrum of the SnS thin film deposited at 27 °C for 24 h. It was seen from the figure that the film contained Sn and S elements. Other elements were also observed due to their presence in the glass substrate. It was found that atomic ratio of Sn/S was 54.13/45.8. EDX analysis showed that the film deposited had almost a stoichiometric composition.

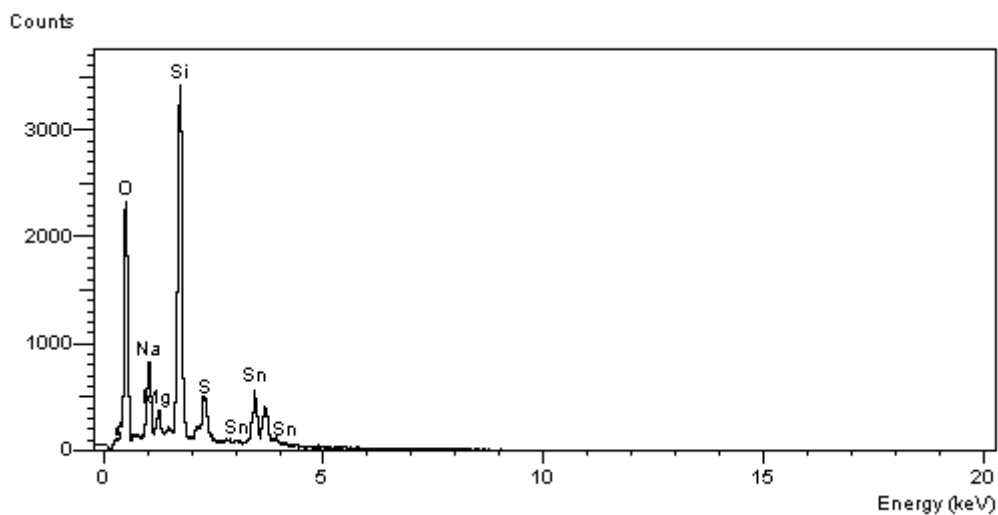


Fig. 3. EDX spectrum of SnS thin film deposited at 27 °C for 24 h.

3. 5. Electrical properties of SnS thin films

It was found that the deposited film has p-type conductivity and its resistivity and mobility were found to be as $2.53 \times 10^5 \Omega \text{ cm}$ and $8.99 \times 10^5 \text{ cm}^2/\text{V.s}$ respectively from the Hall Effect measurements. This resistivity value is in good agreement (10^5 - $10^4 \Omega \text{ cm}$) with Ref. [13] and less ($2.10^6 \Omega \text{ cm}$) than Ref. [14]. As-deposited film was heated to 573 K in order to obtain the temperature-dependence of the electrical conductivity measurements. Then the voltage values were recorded as the temperature was reduced by 5 °C intervals. The obtained experimental data was used in the Arrhenius equation (6) and a change was drawn in Fig. 4 according to $1000/T$ of $\ln(\sigma/\sigma_0)$.

$$\sigma = \sigma_0 e^{-(\Delta E/k_B T)} \quad (6)$$

where σ_0 is a constant, E is the activation energy, k is the Boltzmann constant, T is the absolute temperature and σ is the electrical conductivity.

The activation energy value is one of the most important electrical parameters for materials. From Fig. 4, one region (intrinsic region) is obtained in the temperature range of 353-

573 K. In this region $\ln \frac{\sigma}{\sigma_0}$ increases with increasing temperature. The excitation of the carriers

from the valence band to the conduction band is responsible for this rise of the conductivity where the temperature is high enough. The activation energy value can be calculated from the slope of this curve and it is found to be 0.527 eV. This value was comparable with the previous works [15, 25, 26] and may be attributed to the deep acceptor states stemming from Sn vacancy. This vacancy has an important role in the compounds p-type conductivity. The activation energy value of SnS thin film is dependent on the film thickness, deposition technique and the film composition [5].

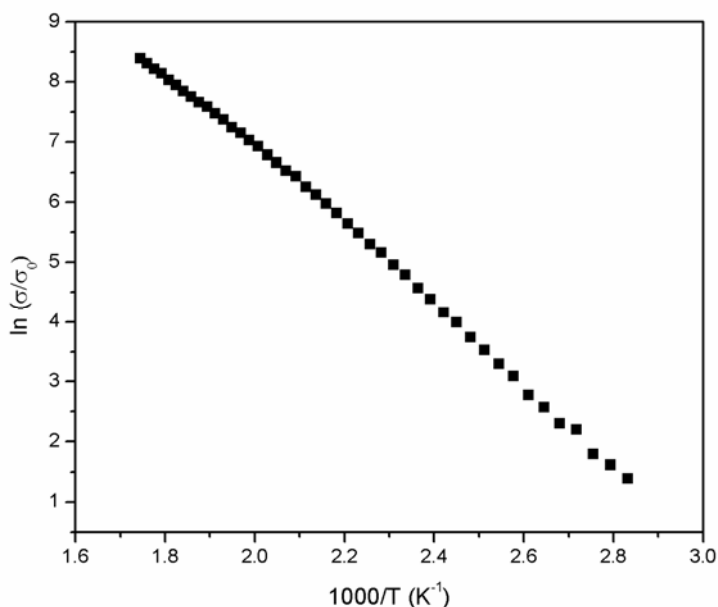


Fig. 4 The dependence of $\ln(\sigma/\sigma_0)$ on $1000/T$ for SnS thin film.

3. 6. The optical properties of SnS thin films

The optical characterization of thin films gives us something about the physical properties such as the band gap energy and band structure etc. [27]. In order to determine these properties optic transition spectrum measurement was performed at room temperature in the wavelength range of 190-1100 nm. The transmittance spectra of the SnS thin film was shown in Fig. 5. In order to estimate the optical band gap, the following equation connecting the photon energy with optic absorption value is used:

$$(\alpha h\nu) \propto (h\nu - E_g)^n \quad (7)$$

where E_g is the energy band gap, α is the absorption coefficient, n is a coefficient having the value 1/2 or 2 depending on the nature of electronic transitions and h is Planck constant. n has the value 1/2 for allowed direct transition, and 2 for allowed indirect transition. Dependence of photon energy on absorption coefficient is an important transition type of electrons and energy band structure. Both direct and indirect gap of the optical transitions at a crystal or polycrystalline depend on material structure. In terms of this, while some scientists have classified optic transition of SnS thin films as direct band gap, others have classified them as indirect. Hence, both direct and indirect values of energy band gap of SnS film were investigated during the study. The point where the linear part of $(\alpha h\nu)^2 = f(h\nu)$ graphic intersects the $h\nu$ axis gives us the forbidden band value for allowed direct transitions; on the other hand, the point where linear part of $(\alpha h\nu)^{1/2} = f(h\nu)$ graphic intersects the $h\nu$ axis gives us the forbidden band value for allowed indirect transitions. From Fig. 6, it was determined that absorption of SnS thin film began at wavelength of 702 nm and reached a maximum value at wavelength of 381 nm. As a result of the fits done on $(\alpha h\nu)^2 - (h\nu)$ and $(\alpha h\nu)^{1/2} - (h\nu)$ graphics we can estimate the allowed direct and indirect energy band values as 1.37 eV [28, 29] and 1.05 eV [29, 30], respectively.

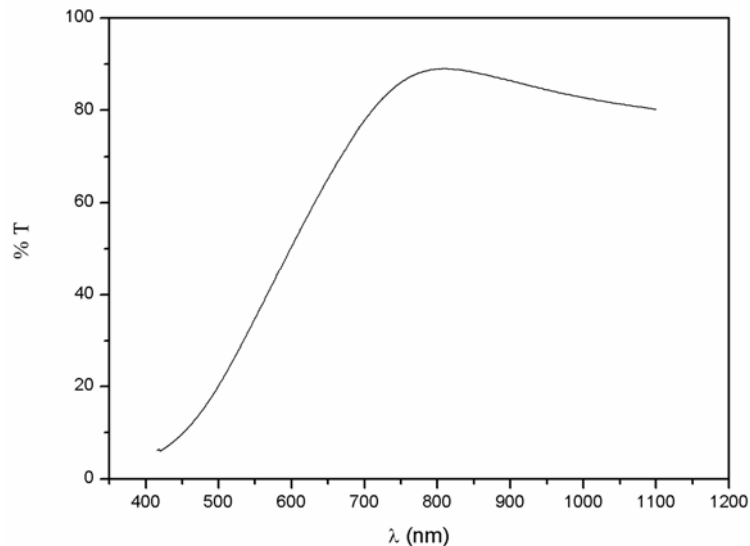


Fig. 5. Optical transmission spectrum for a SnS thin film deposited at 27 °C for 24 h with thickness of 520 nm.

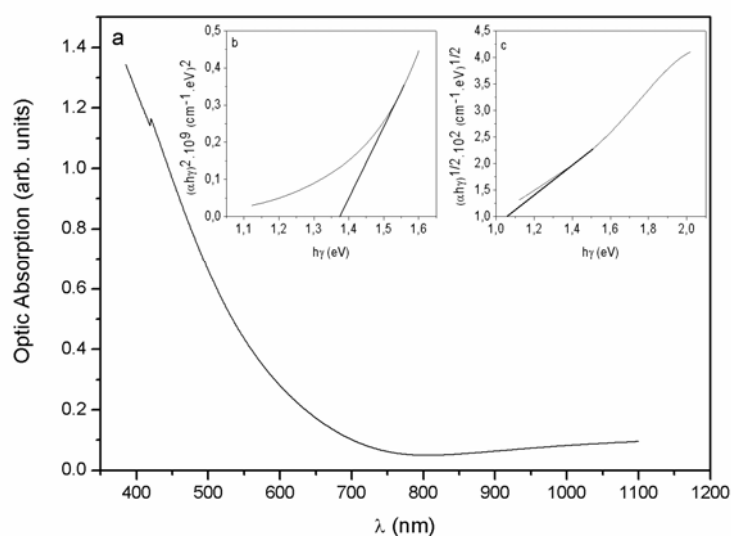


Fig. 6. a) Optic absorption spectrum of SnS thin film deposited at 27 °C for 24 h, b) variation of $(\alpha hv)^2$ versus photon energy ($h\nu$), c) variation of $(\alpha hv)^{1/2}$ versus photon energy ($h\nu$).

4. Conclusions

SnS thin film was successfully deposited onto glass substrates by chemical bath deposition at room temperature for 24 h. The x-ray diffraction spectrum shows that SnS film is polycrystalline with an orthorhombic structure. According to SEM, the thin film on the substrates had good adherence and were free of pinholes. From the EDX result the film was found nearly stoichiometric. The electrical resistivity of SnS thin film was found to be $2.53 \times 10^5 \Omega \cdot \text{cm}$ with a deep impurity level of activation energy of 0.527 eV. The direct and indirect energy band gaps of the film were determined as 1.37 eV and 1.05 eV, respectively. Due to the suitable direct band gap value for an absorber layer for efficient light absorption, SnS thin films can be used as absorber layer in solar cells.

Acknowledgements

We are grateful to Prof. Dr. Mehmet Akkurt from Erciyes University, Faculty of Arts and Sciences, Turkey for his advice. This work was supported by Çukurova University Scientific Research Unit under the project number of FEF2008D18.

References

- [1] E. C. Greyson, J. E. Barton, T. W. Odom, *Small* **2**(3) 368–371 (2006).
- [2] J. B. Johnson, H. Jones, B. S. Latham, J. D. Parker, R. D. Engelken, C. Barber, *Semicond. Sci. Technol.* **14**, 501-507 (1999)
- [3] A. Akkari, C. Guasch, N. Kamoun-Turki, *J. Alloy Compd.* **490**, 180–183 (2010)
- [4] S. Cheng, Y. Chen, C. Huang, G. Chen, *Thin Solid Films* **500**, 96–100. (2006)
- [5] M. Devika, N. Reedy, K. Ramesh, K. Gunasekhar, E. Gopal, K. Reddy, *Semicond. Sci. Technol.* **21**, 1125-1131 (2006)
- [6] D. Avellaneda, G. Delgado, M. Nair, P. Nair, *Thin Solid Films* **515**, 5771–5776. (2007)
- [7] N. Sato, M. Ichimura, E. Araia, Y. Yamazaki, *Sol. Energy Mater. Sol. Cells* **85**, 153 (2005)
- [8] O. E. Ogah, G. Zoppi, I. Forbes, R. W. Miles, *Thin Solid Films* **517**, 2485. (2009)
- [9] G. H. Yue, W. Wang, L. S. Wang, X. Wang, P. X. Yan, Y. Chen, D. L. Peng, *J. Alloy Compd.* **474**, 445 (2009).

- [10] E. Guneri, C. Gumus, F. Mansur, F. Kirmizigul, *Optoelectron. Adv. Mat.* **3**, 383 (2009).
- [11] B. Ghosh, M. Das, P. Banerjee, S. Das, *Appl. Surf. Sci.* **254**, 6436 (2008).
- [12] A. Tanusevski, D. Poelman, *Sol. Energy Mater. Sol. Cells* **80**, 297 (2003).
- [13] M. T. S. Nair, P. K. Nair, *Semicond. Sci. Technol.* **6**, 132 (1991).
- [14] N. K. Reddy, K. T. Ramakrishna Reddy, *Thin Solid Films* **325**, 4 (1998).
- [15] G. Hodes, *Chemical solution deposition of semiconductor films*, Merker Dekker, Inc., New York, 2003, pp. 31-131.
- [16] P. P. Hankare, A. V. Jadhav, P. A. Chate, K. C. Rathod, P. A. Chavan, S. A. Ingole, *J. Alloy Compd.* **463** 581 (2008).
- [17] M. M. El-Nahass, H. M. Zeyada, M. S. Aziz, N. A. El-Ghamaz, *Opt. Mater.* **20**, 159 (2002).
- [18] B. Thangaraju and P. Kaliannan, *J. Phys. D: Appl. Phys.* **33**, 1054 (2000).
- [19] M. Mnari, N. Kamoun, J. Bonnet, M. Dachraoui, *C. R. Chimie* **12**, 824 (2009).
- [20] P. Pramanik, P. K. Basu, S. Biswas, *Thin Solid Films* **150**, 269 (1987).
- [21] B. Cullity, *Elements of X-ray diffraction*, Addison-Wesley Publishing Company Inc., USA, 1967, pp. 501.
- [22] G. Willeke, R. Dasbach, B. Sailer, E. Bucher, *Thin Solid Films* **213**, 271 (1992).
- [23] G. B. Williamson, R. C. Smallman, *Philos. Mag.* **1**, 34 (1956) -46.
- [24] J. Garnier, A. Bouteville, J. Hamilton, M. Pemble, I. Povey, *Thin Solid Films* **518**, 1129 (2009).
- [25] S. Lopez, A. Ortiz, *Semicond. Sci. Technol.* **9**, 2130 (1994).
- [26] M. M. Nassary, temperature dependence of the electrical conductivity, *J. Alloy Compd.* **39**, 21 (2005).
- [27] S. Kasap, P. Capper, *Handbook of electronic and photonic materials*, Springer Science+Business Media, Inc. 2006, pp. 47-74.
- [28] N. K. Reddy, V. Reddy, P. Datta, R. Miles, *Thin Solid Films* **403–404**, 116 (2002).
- [29] A. Tanusevski, *Semicond. Sci. Technol.* **18**, 501 (2003).
- [30] K. Deraman, S. Sakrani, B. Ismail, *SPIE* **2364**, 357 (1994).